Reconstructing long-term (1980–2022) daily ground particulate matter concentrations in India (LongPMInd)

Shuai Wang[1], **Mengyuan Zhang**[1], **Hui Zhao**[2], **Peng Wang**[3,4], **Sri Harsha Kota**[5], **Qingyan Fu**[6], **Cong Liu**[7], **and Hongliang Zhang**[1,4,8]

[1]Department of Environmental Science and Engineering, Fudan University, Shanghai 200438, China
[2]School of Resources and Environmental Engineering,
Jiangsu University of Technology, Changzhou 213001, China
[3]Department of Atmospheric and Oceanic Sciences, Institute of Atmospheric Sciences,
Fudan University, Shanghai 200438, China
[4]IRDR ICoE on Risk Interconnectivity and Governance on Weather/Climate Extremes Impact and Public
Health, Fudan University, Shanghai 200438, China
[5]Department of Civil Engineering, Indian Institute of Technology, Delhi, 110016, India
[6]Shanghai Academy of Environmental Sciences, Shanghai 200003, China
[7]School of Public Health, Fudan University, Shanghai 200032, China
[8]Institute of Eco-Chongming (IEC), East China Normal University, Shanghai 200062, China

Correspondence: Hongliang Zhang (zhanghl@fudan.edu.cn)

Abstract. Severe airborne particulate matter (PM, including $PM_{2.5}$ and PM_{10}) pollution in India has caused widespread concern. Accurate PM concentrations are fundamental for scientific policymaking and health impact assessment, while surface observations in India are limited due to scarce sites and uneven distribution. In this work, a simple structured, efficient, and robust model based on the Light Gradient-Boosting Machine (LightGBM) was developed to fuse multisource data and estimate long-term (1980–2022) historical daily ground PM concentrations in India (LongPMInd). The LightGBM model shows good accuracy with out-of-sample, out-of-site, and out-of-year cross-validation (CV) test R^2 values of 0.77, 0.70, and 0.66, respectively. Small performance gaps between $PM_{2.5}$ training and testing (delta RMSE of 1.06, 3.83, and 7.74 $\mu g\,m^{-3}$) indicate low overfitting risks. With great generalization ability, the openly accessible, long-term, and high-quality daily $PM_{2.5}$ and PM_{10} products were then reconstructed (10 km, 1980–2022). This showed that India has experienced severe PM pollution in the Indo-Gangetic Plain (IGP), especially in winter. PM concentrations have significantly increased ($p < 0.05$) in most regions since 2000 (0.34 $\mu g\,m^{-3}\,yr^{-1}$). The turning point occurred in 2018 when the Indian government launched the National Clean Air Programme, and $PM_{2.5}$ concentrations declined in most regions ($-0.78\,\mu g\,m^{-3}\,yr^{-1}$) during 2018–2022. Severe $PM_{2.5}$ pollution caused continuous increased attributable premature mortalities, from 0.73 (95 % confidence interval (CI) [0.65, 0.80]) million in 2000 to 1.22 (95 % CI [1.03, 1.41]) million in 2019, particularly in the IGP, where attributable mortality increased from 0.36 million to 0.60 million. LongPMInd has the potential to support multiple applications of air quality management, public health initiatives, and efforts to address climate change. The daily and monthly $PM_{2.5}$ and PM_{10} concentrations are publicly accessible at https://doi.org/10.5281/zenodo.10073944 (Wang et al., 2023a).

1   Introduction

Airborne particulate matter (PM, including $PM_{2.5}$ with diameters $< 2.5\,\mu m$ and PM_{10} with diameters $< 10\,\mu m$) not only impacts climate by changing radiation budgets but also has significant adverse effects on human health (Murray et al., 2020; Wang et al., 2012; Yang et al., 2016). India is one of the world's most populous countries, with severe PM pollution resulting from rapid economic development and industrialization over the last few decades. Exposure to $PM_{2.5}$ has become one of the leading causes of health burden in India, contributing to, for example, heart disease, stroke, lung cancer, and premature death (Pandey et al., 2021; Dandona et al., 2017).

Accurate ground PM concentrations are prerequisites for evidence-based policymaking and health impact assessments. The Central Pollution Control Board (CPCB) of India has established and maintained ground-based monitoring networks with ~ 335 continuous ambient air quality monitoring stations (CAAQMSs) currently. However, these monitoring sites are unevenly distributed (mainly located in urban, residential, and industrial areas), with a limited number of sites (monitoring density: ~ 0.6 sites per million population) (Brauer et al., 2019), and many cities even have no monitoring sites (Martin et al., 2019). Therefore, the surface observations alone are not sufficient to support air quality management, especially on a regional scale (Pant et al., 2019; Dey et al., 2020).

Two main approaches have been used for large-scale and long-term $PM_{2.5}$ estimation: scaling methods and statistical methods. Scaling methods use chemical transport models (CTMs) to simulate the association between aerosol optical depth (AOD) and $PM_{2.5}$ and require no ground observations. However, the relationship between $PM_{2.5}$ and AOD is spatially and temporally variable and without the constraints of ground observations, so these methods usually have a large uncertainty (Ma et al., 2022). Compared with scaling methods, statistical methods based on multivariate data fusion have higher prediction accuracy and have been widely used. Statistical models (traditional linear and nonlinear regression and machine learning algorithms) estimate $PM_{2.5}$ concentrations by fitting the relationship between input variables (meteorological factors, emissions, and other relevant variables) and target variables (Wang et al., 2023b; Wei et al., 2021a; X. Ren et al., 2022; Katoch et al., 2023).

Tree-based machine learning (ML) models typically outperform deep learning approaches and traditional machine learning methods in tabular data (e.g., air pollutant observation datasets) and thus have been widely developed and used (Grinsztajn et al., 2022; Sayeed et al., 2022). Wei et al. (2021a) and Li et al. (2021) reconstructed long-term $PM_{2.5}$ data records in China by fusing satellite, meteorological, and emission data using a spatiotemporal tree-based model. Ni et al. (2024) analyzed the contribution of meteorology and emissions to O_3 in China using a chemical transport model

(GEOS-Chem) and a tree-based model. Sayeed et al. (2022) improved analysis of the $PM_{2.5}$ concentration in the continental United States using the random forest approach coupled with meteorology and aerosol species of the Modern-Era Retrospective analysis for Research and Applications, Version 2 (MERRA-2).

Some studies have estimated $PM_{2.5}$ concentrations in India using different methods. Chowdhury et al. (2019) used the $PM_{2.5}$–AOD equation method to estimate $PM_{2.5}$ concentrations in Delhi; however, AOD satellite data suffer from significant non-random misses, especially during cloud cover and on hazy, polluted days, so it is difficult to derive a full-spatiotemporal-coverage PM dataset (Wang et al., 2023b; Bai et al., 2022). Bali et al. (2021) and Dey et al. (2020) estimated total $PM_{2.5}$ in India through empirical coefficients and the MERRA-2 dataset, but these coefficients vary with geographic location and pollution scenarios, which makes the related estimation potentially unreliable. Kumar et al. (2023) analyzed $PM_{2.5}$ for India using a random forest model and showed a gap between train and test scores with a risk of overfitting. In addition, global-scale daily $PM_{2.5}$ concentration datasets (including India) have recently been developed, including GlobalHighAirPollutants (GHAP) (Wei et al., 2023) and the Long-term Gap-free High-resolution Air Pollutants concentration dataset version 2 (LGHAPv2) (Bai et al., 2024). Global monthly $PM_{2.5}$ datasets have also been developed before (Van Donkelaar et al., 2021). These datasets were trained on a global scale and estimated $PM_{2.5}$ concentrations for the India region. The severity of $PM_{2.5}$ pollution in India is much higher than in Europe and the United States (Wei et al., 2023). However, due to the small number of observations recorded, the global model can gain only limited knowledge of $PM_{2.5}$ pollution in India during the training process. Therefore, the reliability and robustness of global model estimates of $PM_{2.5}$ concentrations in India should be systematically assessed. Building a model locally in India can provide a useful comparison, which can also complement the biases in global modeling (e.g., due to focusing more on lightly polluted regions such as Europe and the United States). However, it is challenging to establish long-term, full-coverage, high-accuracy, open-source PM data products locally in India due to insufficient observational data and lack of model robustness because of variations in data distribution across regions and years (Kumar et al., 2023; Dey et al., 2020).

To improve performance, previous models have usually had high complexity, such as numerous trees and leaf nodes (Zhang et al., 2021; Huang et al., 2021). This practice increases the computational resource requirement and is prone to overfitting, leading to a large gap between the performance of the training and testing data (Zhang et al., 2021; Jabbar and Khan, 2015; Ying, 2019). Therefore, it is necessary to minimize model complexity to avoid overfitting. The Light Gradient-Boosting Machine (LightGBM) is an optimized gradient boosting decision tree (GBDT) (Ke et al.,

2017), and it has shown superior performance in many fields (Wei et al., 2021b; Yan et al., 2021; Sun et al., 2020; Liang et al., 2020). LightGBM uses a histogram-based decision tree algorithm along with gradient-based one-side sampling (GOSS), which can save memory and computation time (Ke et al., 2017). Our previous study comparing several commonly used machine learning models found that LightGBM has similar performance to the eXtreme Gradient Boosting (XGBoost) with the highest accuracy, but LightGBM was faster and more robust, with the potential to estimate long-term concentrations of PM in India (Wang et al., 2023c).

In this work, a simple structured, efficient, and robust model based on LightGBM was developed to estimate PM concentration. Three cross-validation methods and separate test datasets were designed to evaluate model performance. Long-term (1980–2022) and open-source datasets with a spatial resolution of 10 km of $PM_{2.5}$ and PM_{10} in India were then generated, and the mortalities due to $PM_{2.5}$-induced diseases were also estimated. The concentration datasets could help with pollution formation analysis, assessment of PM health risks, and air quality management in India.

2 Materials and methods

2.1 Data sources

Table 1 shows the multisource datasets used in this study. Ground observations of $PM_{2.5}$ and PM_{10} during 2018–2022 in India were collected from the CPCB air quality monitoring network (https://www.cpcb.nic.in, last access: 29 July 2024). The location of monitoring sites is shown in Fig. S1 in the Supplement. As extreme values affect model robustness, the bottom and top 0.01 % of observation data were excluded. The fifth-generation ECMWF atmospheric reanalysis dataset ERA5-Land covering 1980–2022 was used. Features were selected by their relative importance, which was calculated by their gain, and several meteorological factors with high relative importance were included (Table 1). Data products of the Modern-Era Retrospective analysis for Research and Applications, Version 2 (MERRA-2), covering 1980–2022 were also collected, with data including aerosol optical depth and aerosol components and precursors (black carbon, organic carbon, sulfate, dust, and SO_2).

2.2 Model building

In this study, LightGBM (Ke et al., 2017), an efficient gradient boosting decision tree (GBDT), was used to estimate $PM_{2.5}$ and PM_{10}, which has been proven to be accurate, fast, and robust in our previous studies (Wang et al., 2023c, d). A grid search cross-validation (CV) method was used to select the optimal hyperparameters. An algorithm for hyperparameter selection (Algorithm S1 in the Supplement) was designed to ensure the model's generalization ability. Looping is performed to increase the model complexity (e.g., num-

ber of trees), followed by ending the loop and returning the hyperparameters when the model-predicted RMSE does not decrease significantly (< 0.01) or the difference between the training and predicted RMSE does not increase significantly (< 0.05). Features were selected based on their relative importance. Ten meteorological features, six emission-related features, and total aerosol extinction were used to train LightGBM and estimate PM concentrations (Fig. 1). The meteorological and emission features contributed 64 % and 31 % to the $PM_{2.5}$ prediction.

Meteorology is more important than emissions. Compared to MERRA-2, which has higher uncertainty and lower spatial resolution, ERA5 has higher resolution and accuracy, and its meteorological features can provide richer information and contribute more in model training and thus have higher importance (Muñoz-Sabater et al., 2021; Hersbach et al., 2020). Besides, more meteorological features were used to train the model, thus contributing more to prediction results. The highest importance of surface pressure can be attributed to the important effect on $PM_{2.5}$ concentration and its high data quality (Chen et al., 2020; Bauer et al., 2015).

Three independent CV methods and three metrics (coefficient of determination: R^2; root mean square error: RMSE; mean absolute error: MAE) were designed to evaluate the model's spatiotemporal predictive power. The first is out-of-sample CV, where the dataset is randomly divided into 10 subsets, 1 of which is taken in turn for testing and the remaining 9 of which are used for training; this is repeated 10 times and averaged. The second is out-of-site CV, which is similar to the out-of-sample CV, but the dataset is randomly divided by site. This method can measure the model's spatial predictive power. The third method is interannual out-of-year CV, which sequentially takes 1 year of data for testing and the rest for training. This approach can measure the model's predictive power for the years with no observations. Besides, observations in January–June 2023 were used as a separate test set, and these data were not involved in any of the training and hyperparameter selection processes.

2.3 Mortality estimation

According to the database of the Global Burden of Disease (GBD) study in 2019 (Murray et al., 2020; Vos et al., 2020), annual average concentrations were used to assess long-term exposure to $PM_{2.5}$, and premature deaths were assessed using the following equation:

$$M_{y,i,j} = \frac{RR_j(C_{y,i}) - 1}{RR_j(C_{y,i})} \times P_{y,i} \times I_{y,j}, \tag{1}$$

where $M_{y,i}$ represents the mortality attributable to cause j due to long-term $PM_{2.5}$ exposure in year y in region i, $RR(C_{y,i})$ represents the relative risk of cause j for year y in region i, $P_{y,i}$ represents the population j in year y in region i, and I_y represents the baseline mortality in year y.

Table 1. Summary of the ERA5, MERRA-2, and ground observation data used in this study.

Type	Variable	Description	Spatial resolution	Temporal resolution
ERA5	SSRD	Surface solar radiation	$0.1° \times 0.1°$	Hourly
	BLH	Boundary layer height	$0.25° \times 0.25°$	Hourly
	EVAP	Evaporation	$0.1° \times 0.1°$	Hourly
	TEMP2	2 m air temperature	$0.1° \times 0.1°$	Hourly
	DEWP2	2 m dew point temperature	$0.1° \times 0.1°$	Hourly
	SP	Surface pressure	$0.1° \times 0.1°$	Hourly
	TPREC	Total precipitation	$0.1° \times 0.1°$	Hourly
	TCLOUD	Total cloud cover	$0.25° \times 0.25°$	Hourly
	UWIND10	10 m u component of wind	$0.1° \times 0.1°$	Hourly
	VWIND10	10 m v component of wind	$0.1° \times 0.1°$	Hourly
MERRA-2	BCSMASS	Black carbon surface mass concentration	$0.5° \times 0.625°$	Hourly
	OCSMASS	Organic carbon surface mass concentration	$0.5° \times 0.625°$	Hourly
	DUSMASS25	Dust $PM_{2.5}$ surface mass concentration	$0.5° \times 0.625°$	Hourly
	DUSMASS	Dust surface mass concentration	$0.5° \times 0.625°$	Hourly
	SO2SMASS	Sulfur dioxide surface mass concentration	$0.5° \times 0.625°$	Hourly
	SO4SMASS	Sulfate surface mass concentration	$0.5° \times 0.625°$	Hourly
	TOTEXTTAU	Total aerosol extinction [550 nm]	$0.5° \times 0.625°$	Hourly
Observation	$PM_{2.5}$, PM_{10}	Particulate matter	Point	Hourly
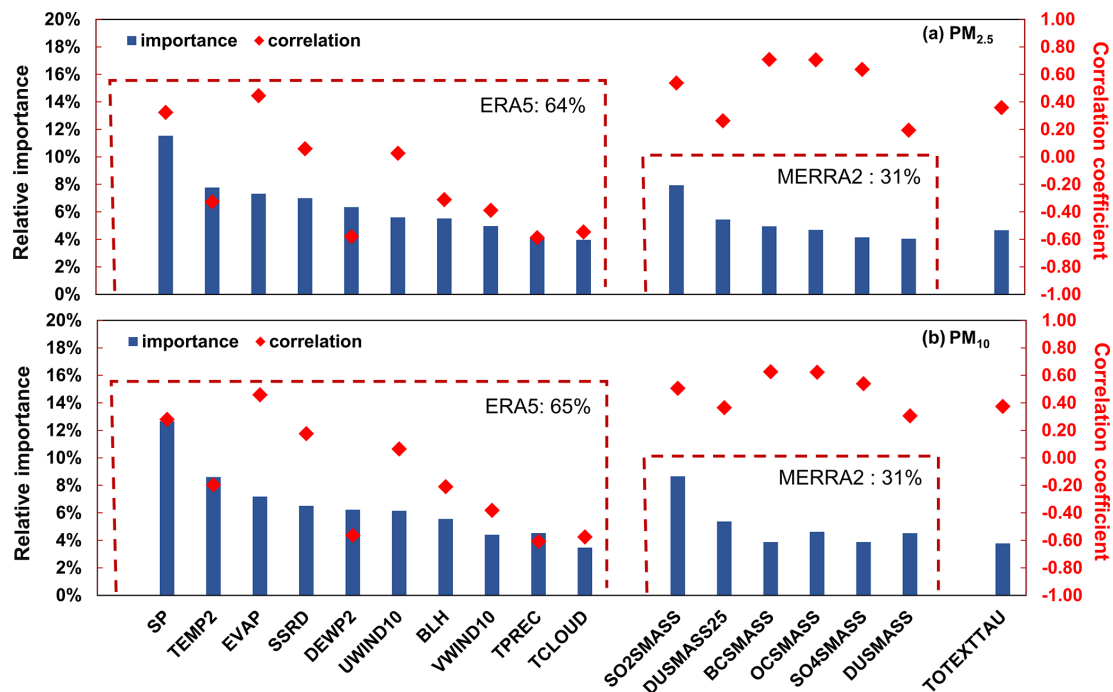
Figure 1. Relative importance and correlation coefficient for the $PM_{2.5}$ and PM_{10} estimate models. A description of the features is given in Table 1.

$PM_{2.5}$ exposure-related deaths due to ischemic heart disease (CVD_IHD), chronic stroke (CVD_stroke), obstructive pulmonary disease (RESP_COPD), lung cancer (NEO_LUNG), lower respiratory infections (LRI), and type 2 diabetes mellitus (T2_DM) were estimated. The gridded population data were obtained from WorldPop datasets (https://www.worldpop.org, last access: 29 July 2024). The relative risk is a discrete value obtained from GBD 2019 and is the relative risk corresponding to each $PM_{2.5}$ concentration level. Details about the calculation of relative risk can be found in GBD 2019 (Murray et al., 2020). Annual baseline mortality (2000–2019) and the risk of cause-specific deaths

Table 2. Summary of the LongPMInd dataset.

Data description	LongPMInd dataset
Data type	Gridded
File format	NetCDF
Species	$PM_{2.5}$, PM_{10}
Spatial reference	WGS 84
Horizontal resolution	$0.1° \times 0.1°$ ($\approx 10\,km \times 10\,km$)
Horizontal coverage	India ([5.0° N, 40.0° N], [60° E, 100° E])
Temporal resolution	Daily, monthly, and yearly
Temporal coverage	1980–2022

at different $PM_{2.5}$ levels were obtained from GBD 2019. The minimum-risk exposure level for the health effects of $PM_{2.5}$ is in the range of 2.4 to $5.9\,\mu g\,m^{-3}$.

3 Data availability

The LongPMInd dataset, including daily $PM_{2.5}$ and PM_{10} concentration (10 km) for India during 1980–2022, is publicly accessible. All data are provided in NetCDF format and can be downloaded at https://doi.org/10.5281/zenodo.10073944 (Wang et al., 2023a).

4 Results

4.1 Long-term India $PM_{2.5}$ dataset

Applying the trained LightGBM model to the large input dataset constructed for the years 1980–2022, the long-term high-quality daily $PM_{2.5}$ and PM_{10} products of India (LongPMInd) are reconstructed. Table 2 summarizes basic information about the dataset; the data are provided in NetCDF format with a spatial resolution of 10 km. The LongPMInd dataset, to the best of our knowledge, is the first open-source, long-term (i.e., 1980–2022), and relatively high accuracy dataset covering the whole of India. The daily, monthly, and yearly $PM_{2.5}$ and PM_{10} datasets are publicly available at https://doi.org/10.5281/zenodo.10073944 (Wang et al., 2023a).

4.2 Model performance

Table 3 shows the training and testing results of out-of-sample CV, out-of-site CV, and out-of-year CV for daily $PM_{2.5}$ and PM_{10}. Overall, the model shows good accuracy, with out-of-sample CV R^2 values of 0.77 and 0.76 and RMSE of 29.57 and $51.63\,\mu g\,m^{-3}$ for daily $PM_{2.5}$ and PM_{10}. Monthly predictions show better performance, with out-of-sample CV R^2 values of 0.87 and 0.86 and RMSE of 17.65 and $31.26\,\mu g\,m^{-3}$ for monthly $PM_{2.5}$ and PM_{10}. More importantly, out-of-sample CV results of training and testing showed small accuracy gaps with RMSE and MAE of 1.06 (4 %) and 0.51 (3 %) $\mu g\,m^{-3}$ for $PM_{2.5}$ and 1.52 (3 %)

and 0.9 (3 %) $\mu g\,m^{-3}$ for PM_{10}, reflecting good generalization ability. Out-of-site CV measures the model's predictive ability for unobserved areas. The spatially validated R^2 and RMSE for $PM_{2.5}$ and PM_{10} were 0.70 and 0.65 and 31.73 and $51.37\,\mu g\,m^{-3}$, respectively, indicating the model's ability to fill the unobserved areas accurately. The small performance gap between out-of-site CV training and testing also reflects good spatial generalization ability. Observations before 2018 are limited due to the number and quality of sites. Out-of-year CV was used to evaluate LightGBM prediction performance, which was conducted by sequentially taking 1 year of data for testing and the rest for training. The model's prediction accuracy for unobserved years decreases slightly compared to out-of-sample CV (R^2 decreases by 14 %, and RMSE increases by 20 %) due to differences in data distributions among years (Fig. S2). Notably, most predictions are consistent with observations, with most data samples evenly distributed around the 1 : 1 line (Fig. S3) but with underestimation for high PM levels and overestimation for low PM levels (slopes of 0.75 and 0.74 and intercepts of 16.45 and $35.79\,\mu g\,m^{-3}$ for daily $PM_{2.5}$ and PM_{10} predictions). Monthly predictions show better agreement with observations, with slopes of 0.84 and 0.82 and intercepts of 10.26 and $23.53\,\mu g\,m^{-3}$ for monthly $PM_{2.5}$ and PM_{10}. The underestimation and overestimation indicate the potential unreliability of model predictions for extreme pollution and extreme clean days. This can be attributed to the small proportion of data records for extreme pollution and clean days.

Observations from January to June 2023 were used for testing and were not involved in any training or hyperparameter selection processes (Fig. S4 and Table S1 in the Supplement). Six representative regions were selected for the analysis including Delhi and Uttar Pradesh (the Indo-Gangetic Plain – IGP – region), Gujarat (western India region), Madhya Pradesh (central India region), West Bengal (eastern India region), and Andhra Pradesh (southern India region). The model shows accurate prediction ability with RMSE of 33.58 and $64.25\,\mu g\,m^{-3}$ for $PM_{2.5}$ and PM_{10}, respectively, in India. The model can capture the decreasing trend in PM concentration from January to June in different regions of India but with some biases, e.g., overestimation of $PM_{2.5}$ in Uttar Pradesh on 8 January and underestimation of haze pollution in Gujarat on 19 February. The large RMSE of $PM_{2.5}$ prediction in Uttar Pradesh ($32.72\,\mu g\,m^{-3}$) could be attributed to the complexity of pollution causes in the region as well as insufficient observation data. The small RMSE ($8.34\,\mu g\,m^{-3}$) of $PM_{2.5}$ prediction in Andhra Pradesh can be related to the light haze pollution and small fluctuation in $PM_{2.5}$ concentration.

4.3 Spatial and temporal trends

First, spatial patterns of $PM_{2.5}$ and PM_{10} are analyzed (Figs. S5 and S6). The Indo-Gangetic Plain (IGP) and western arid regions show high levels of $PM_{2.5}$ and PM_{10}, es-

Table 3. Training and testing results of out-of-sample CV, out-of-site CV, and out-of-year CV for daily $PM_{2.5}$ and PM_{10} (2018–2022). RMSE and MAE unit: $\mu g\,m^{-3}$.

Species	Type	R^2		RMSE ($\mu g\,m^{-3}$)		MAE ($\mu g\,m^{-3}$)	
		Test	Train	Test	Train	Test	Train
$PM_{2.5}$	out-of-sample	0.77	0.79	29.57	28.51	18.76	18.25
	out-of-site	0.70	0.79	31.73	27.90	20.32	17.78
	out-of-year	0.66	0.79	35.35	27.61	21.54	17.61
PM_{10}	out-of-sample	0.76	0.77	51.63	50.11	35.42	34.52
	out-of-site	0.65	0.77	57.37	49.42	39.92	33.94
	out-of-year	0.66	0.78	60.65	49.06	40.74	33.72

pecially for years after 2000. Low PM concentrations were observed in southern India. The high terrain in the northern and southern IGP is unfavorable for pollutant dispersion. Intense human activities in the IGP (population > 700 million) emit large quantities of primary PM and gas pollutants (SO_2 and nitrogen oxide), and this, coupled with unfavorable dispersion conditions, leads to severe PM pollution (Dey et al., 2020; Maheshwarkar et al., 2022). Both $PM_{2.5}$ and PM_{10} concentrations show a north-to-south (high-to-low) distribution, consistent with the population distribution and corresponding anthropogenic emissions (Upadhyay et al., 2020; Dey et al., 2020).

Figure 2 shows the spatial patterns of seasonal $PM_{2.5}$ and PM_{10} anomalies. The highest PM levels occurred in winter, especially in the IGP (positive anomaly > $20\,\mu g\,m^{-3}$ relative to the annual mean during 1980–2022). This enhancement is related to additional anthropogenic emissions (from space and water heating of households especially in cold places like the IGP) and stable meteorological conditions (low boundary layer height and low wind speed) (Pandey et al., 2014; Tiwari et al., 2013). During the pre-monsoon season (March–April–May), favorable meteorological conditions (increased boundary layer height due to increased temperature and wind speeds) reduce $PM_{2.5}$ concentrations in the IGP area (Dey et al., 2020). During the monsoon season (June to September), rainfall enhances PM deposition, resulting in a substantial reduction in PM concentrations. With the end of the monsoon (post-monsoon season, October and November), less rainfall, lower temperatures, extensive open biomass burning (for heating), and reduced boundary layer heights exacerbate PM pollution (Nagpure et al., 2015; Kumari et al., 2021).

The long-term trends of aerosols in India can be better examined given the advantage of long temporal coverage of the LongPMInd dataset. The monthly $PM_{2.5}$ and PM_{10} anomalies from 1980 to 2022 in India and typical regions were first calculated (Figs. 3 and S7). PM concentrations slowly increased in India ($0.19\,\mu g\,m^{-3}\,yr^{-1}$) before 2000; in the IGP and eastern India, they increased by 0.43 and $0.26\,\mu g\,m^{-3}\,yr^{-1}$, respectively. The PM concentrations jumped in 2000, which can be attributed to the absence of

satellite data for MERRA-2 before 2000 (Buchard et al., 2017). The MERRA-2 dataset before 2000 could not provide the same level of data quality as in the later period, further leading to a systematic bias in the model estimates. With accelerated industrialization, anthropogenic emissions of primary particulate matter (PPM) and precursors of secondary aerosols (e.g., SO_2, NO, and NH_3) have increased since 2000 (Pandey et al., 2014; Nagpure et al., 2015), leading to significant increases in PM concentrations in most regions ($p < 0.05$), except for western India (Figs. 4 and S8). $PM_{2.5}$ increased by 0.50 and $0.46\,\mu g\,m^{-3}\,yr^{-1}$ in the IGP and eastern India during 2000–2017. In early 2018, the Indian government launched the National Clean Air Programme (NCAP). The interventions were grouped into transport, industry, waste management, domestic, and construction activities as well as road dust and others (Ganguly et al., 2020). Emissions declined rapidly, and $PM_{2.5}$ concentrations declined significantly in the IGP ($1.63\,\mu g\,m^{-3}\,yr^{-1}$), western India ($1.22\,\mu g\,m^{-3}\,yr^{-1}$), and southern India ($0.52\,\mu g\,m^{-3}\,yr^{-1}$). However, PM concentrations in east-central India showed an increasing trend (Fig. 4), which may be related to emissions from mining activities and related industries and thermal power plants (Upadhyay et al., 2020).

4.4 Health burden analysis

The health burden of $PM_{2.5}$ was estimated from 2000–2019 following the rapid increase in $PM_{2.5}$ concentrations after 2000. Using GBD 2019, premature deaths attributed to $PM_{2.5}$ exposure were calculated for six diseases, comprising ischemic heart disease (CVD_IHD), chronic stroke (CVD_stroke), obstructive pulmonary disease (RESP_COPD), lung cancer (NEO_LUNG), lower respiratory infections (LRI), and diabetes mellitus type 2 (T2_DM) (Murray et al., 2020; Vos et al., 2020).

Figure 5 shows the changes in annual average $PM_{2.5}$ concentrations and corresponding attributed deaths, and Table S2 shows the related uncertainties. $PM_{2.5}$ concentrations showed a fluctuating upward trend with a continuous increase in attributable premature mortality, from 0.73 (95 % confidence interval (CI) [0.65, 0.80]) million prema-
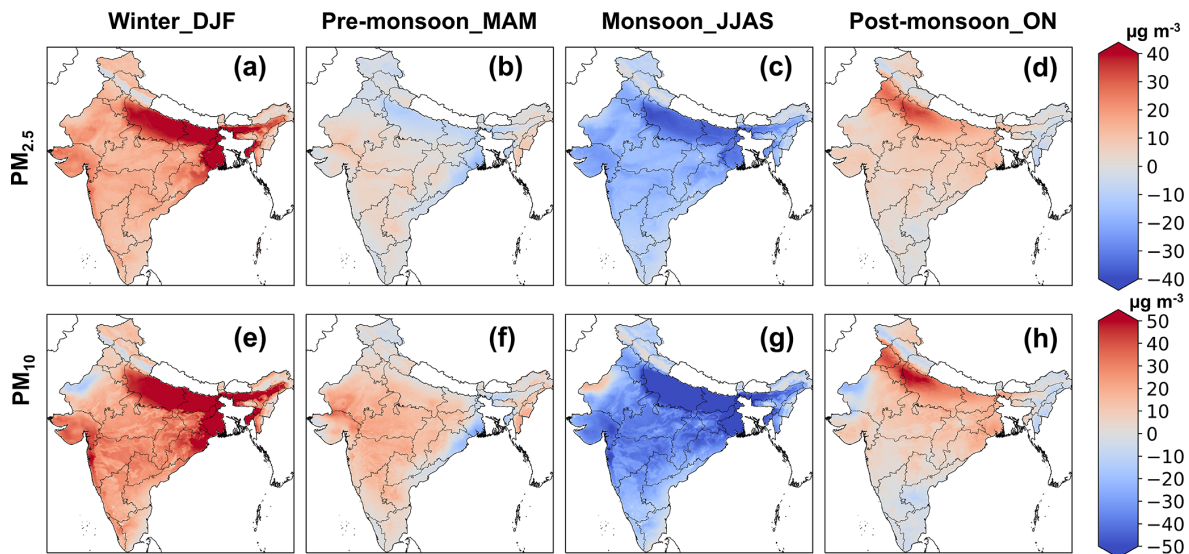
Figure 2. Spatial patterns of seasonal $PM_{2.5}$ and PM_{10} anomalies (the difference between the seasonal mean and annual mean) in India during 1980–2022.
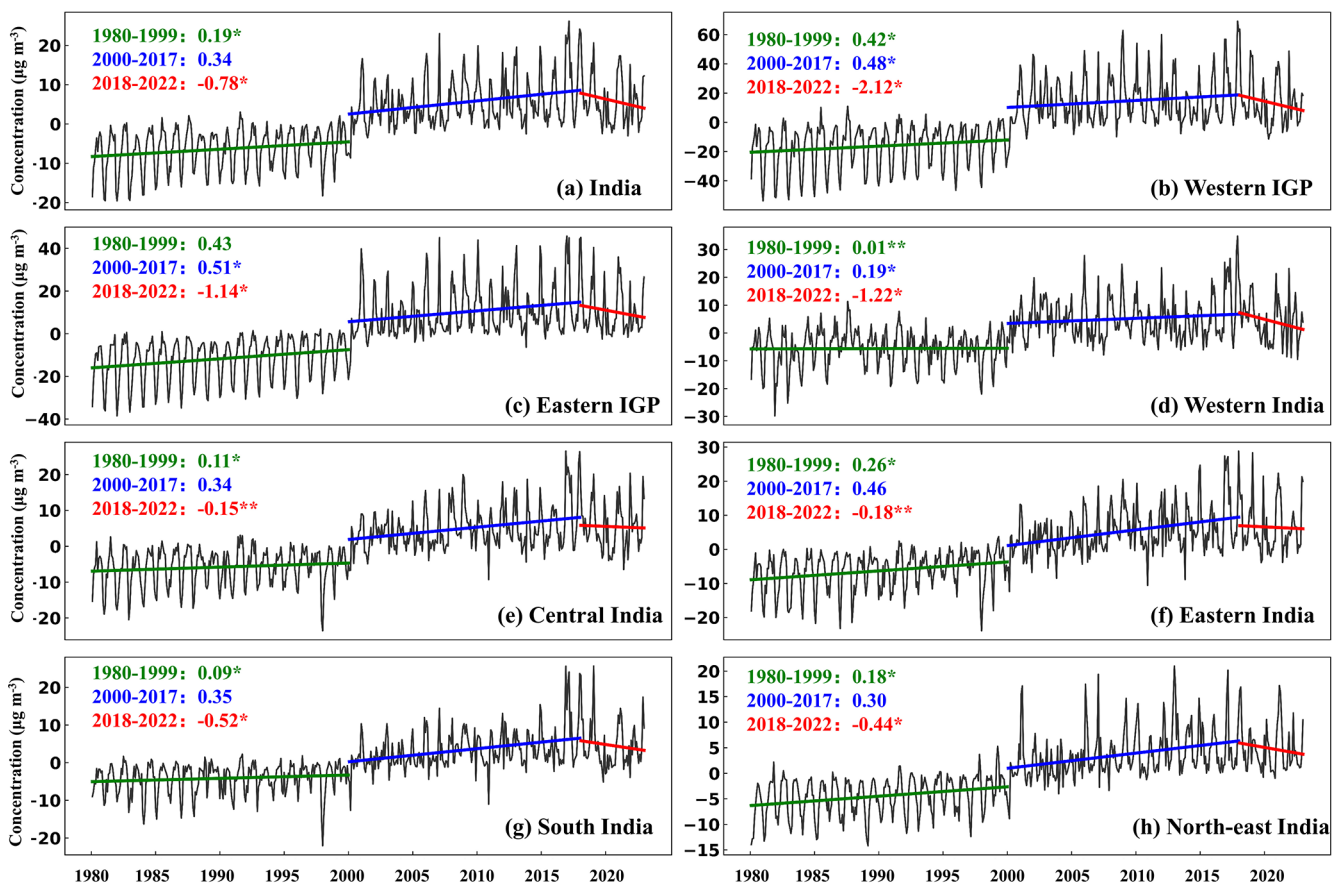
Figure 3. Time series of the monthly $PM_{2.5}$ anomaly from 1980 to 2022 in India (overall and regionally). The colored straight lines are the linear regression trend ($\mu g\,m^{-3}\,yr^{-1}$) for different periods in China, and * represent the significance of the trends (* mean $p < 0.05$ and ** mean $p < 0.01$).
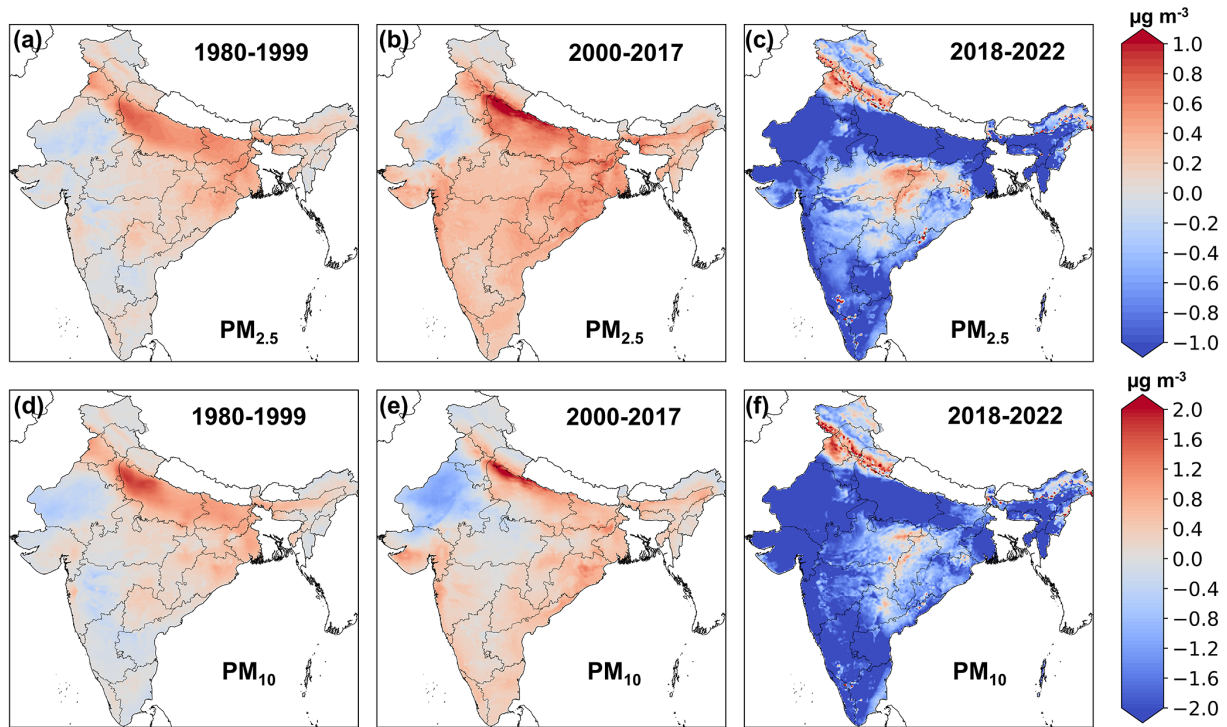
Figure 4. Spatial patterns of annual changes for $PM_{2.5}$ and PM_{10} ($\mu g\,m^{-3}\,yr^{-1}$) during different periods (1980–1999, 2000–2017, and 2018–2022). Publisher's remark: please note that the above figure contains disputed territories.

ture deaths in 2000 to 1.22 (95 % CI [1.03, 1.41]) million in 2019, with CVD_IHD, CVD_stroke, RESP_COPD, NEO_LUNG, LRI, and T2_DM causing an annual average of 0.35 million, 0.21 million, 0.21 million, 0.02 million, 0.12 million, and 0.04 million premature deaths, respectively. $PM_{2.5}$-attributable deaths were counted by region (Fig. 5). The IGP had the highest attributable premature deaths, increasing from 0.36 million in 2000 to 0.60 million in 2019, due to high population density coupled with severe haze pollution (Dey et al., 2020; Pandey et al., 2021).

To reduce premature deaths from $PM_{2.5}$ exposure, policies to mitigate $PM_{2.5}$ pollution should be implemented. In addition, appropriate health advice and enhanced medical facilities to reduce baseline mortality are also important to reduce the health burden (Maji et al., 2023). India has experienced rapid urbanization and large-scale population migration, which introduces uncertainty into health risk estimates for $PM_{2.5}$ (Shi et al., 2020). Country-level baseline disease rates were used, so regional differences were not accounted for due to lack of data, which could introduce some error. In addition, uncertainties in relative risk, population, and $PM_{2.5}$ concentrations may also introduce errors into health risk estimates.
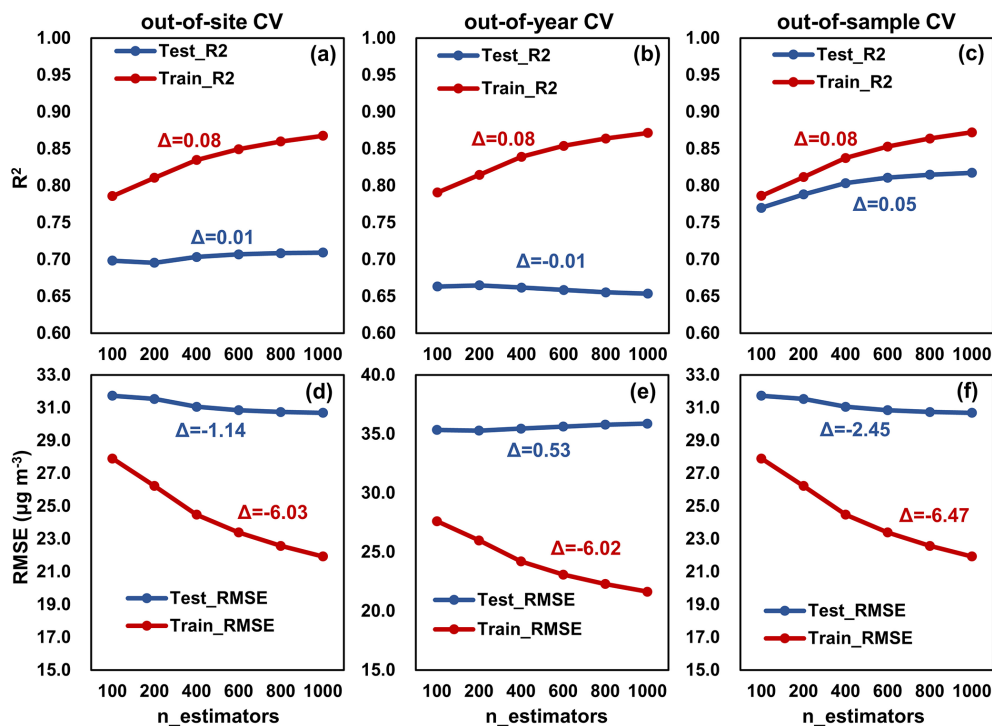
4.5 Model complexity

Model complexity can be measured by the number of parameters the model has. As model complexity increases, the
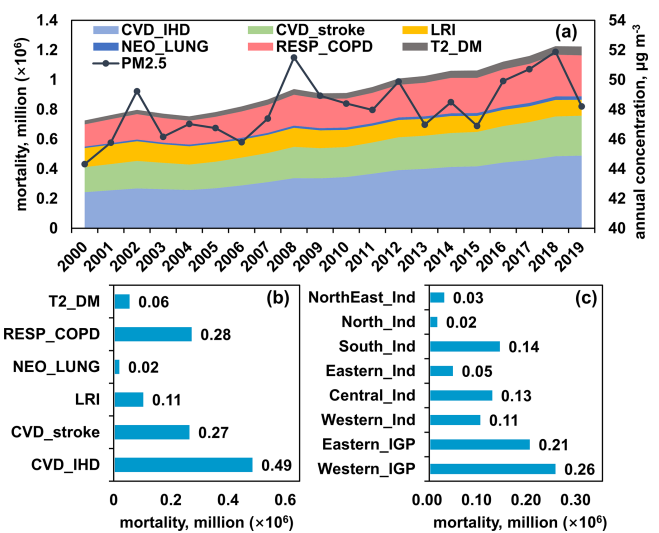
Figure 5. Annual mortalities due to $PM_{2.5}$-induced diseases in India during 2000–2019, including ischemic heart disease (CVD_IHD), chronic stroke (CVD_stroke), obstructive pulmonary disease (RESP_COPD), lung cancer (NEO_LUNG), lower respiratory infections (LRI), and diabetes mellitus type 2 (T2_DM). Panels (b) and (c) show statistical results for causes and regions.

Figure 6. Three CV results of the model complexity test for $PM_{2.5}$ estimation. The n_estimators is the number of trees, representing the complexity of LightGBM. Δ is the difference between the metrics with n_estimators = 1000 and n_estimators = 100. Units of RMSE and MAE are $\mu g\,m^{-3}$.

model is more capable of learning complex patterns in the data, but at the same time, it may lead to overfitting and inaccurate predictions of new and unseen data (Hu et al., 2021). The impact of the complexity of the tree-based LightGBM model on the performance of training and testing is analyzed (Fig. 6). The number of trees (n_estimators) was used as a complexity proxy, and the other hyperparameters were kept constant. All three cross-validation results show that the increase in model complexity improves the model's fitting ability, increasing R^2 and decreasing RMSE. However, the increase in complexity did not improve the model's predictive performance. With n_estimators increasing from 100 to 1000, there was no significant change in R^2 for the out-of-site and out-of-year CV (−0.01 to 0.01), and the RMSE for the out-of-year CV on the contrary increased by 0.53. Out-of-sample CV showed an improvement in R^2 but with a limited reduction in RMSE (−2.45). Therefore, using only out-of-sample CV to select hyperparameters and evaluate the model is limiting, and out-of-site and out-of-year CV allows a more objective evaluation of the model's generalization ability.

4.6   Uncertainties

Uncertainty in this study comes from two main sources: the machine learning model and the dataset used. Firstly, machine learning is essentially based on probability theory and is influenced by the distribution pattern of the target variable

$(PM_{2.5}$ and $PM_{10})$ (Yang et al., 2021; Breiman, 2001). Due to the low frequency of extreme pollution scenarios, the model suffers from the problem of smoothing predictions, i.e., underestimating high-pollution scenarios (Wei et al., 2021a; Yu et al., 2023; Geng et al., 2021). In addition, machine learning has limitations in describing atmospheric physical and chemical processes, and it is difficult to fit complex, logistically long processes, such as secondary aerosol generation (Stirnberg et al., 2021; Li et al., 2023). Attempts have been made to incorporate physical constraints into neural networks to improve interpretability, but this approach is limited to spatially continuous two-dimensional data (Geiss et al., 2022). Other studies have shown that chemical reaction processes can be described by neural networks, but it is still a challenge to efficiently couple them with CTMs (Huang et al., 2022; Huang and Seinfeld, 2022).

The second aspect is the uncertainties caused by the datasets. First, the label (observations) and corresponding features (MERRA-2 and ERA5) have a long-tailed distribution with few high-pollution records, so there is an issue of imbalance regression (Yang et al., 2021). The model was trained with a bias towards denser observations, leading to the underestimation of high-pollution scenarios. For the problem of imbalanced regression, there are currently mainly data-based solutions and model-based solutions (J. Ren et al., 2022). Data-based solutions require acquiring more data or

changing the data distribution by resampling. Model-based solutions increase the weighting of fewer samples (high-pollution scenarios) by modifying the loss function. Both methods can improve the accuracy of fewer samples, but they are not suitable for the task of this study because the distribution of the data was altered. Therefore, more observations should be collected in the future to increase observations recorded for high-pollution scenarios and mitigate the problem of imbalanced regression. In addition, observational data can only be collected for recent years (2018–2022), which may lead to uncertainties when inferring PM concentrations for historical years. In out-of-year validation, the gap between training and testing is mainly attributed to the difference in the data distribution among years (data drift, Fig. S2). Besides, changes in climate and human activities over the decades may affect the relationship among emissions, meteorology, and PM concentrations, resulting in extra uncertainty (concept drift).

Secondly, the uncertainty in the input feature sets (ERA5 and MERRA-2) also affects the estimation results. The uncertainty in ERA5, a widely used meteorological reanalysis dataset, has been systematically analyzed. ERA5 has good accuracy for most meteorological factors, exceeding other reanalysis data (Muñoz-Sabater et al., 2021; Hersbach et al., 2020). With MODIS data as a reference, the global mean surface temperature of ERA5-Land shows lower uncertainty (Muñoz-Sabater et al., 2021). For precipitation, ERA5 shows 77 % correlation with monthly mean Global Precipitation Climatology Project (GPCP) data (Hersbach et al., 2020). Compared to the pre-assimilation data, ERA5-Land provides an improved fit to tropospheric winds and humidity (Hersbach et al., 2020).

MERRA-2 is a global air pollution reanalysis dataset, published and maintained by NASA; it has been widely used for PM pollution studies in the Indian region, and its reliability has been extensively analyzed (Gueymard and Yang, 2020; Navinya et al., 2020; Buchard et al., 2017). For MERRA-2 AOD, evaluation using AERONET observations showed that MERRA-2 outperformed the Copernicus Atmosphere Monitoring Service (CAMS) in most regions (Gueymard and Yang, 2020). Kumar et al. (2023) predicted ground-level $PM_{2.5}$ concentrations in India using only MERRA-2 and machine learning methods, proving the reliability of MERRA-2 data.

In addition, before 2000, there were no assimilated satellite data for MERRA-2, and nitrate was not provided in the MERRA-2 aerosol reanalysis datasets (Buchard et al., 2017). These issues may be detrimental to the accuracy of the LongPMInd dataset. Previous studies in India have shown that $PM_{2.5}$ estimates based on MERRA-2 and empirical formulas suffer from inaccuracies due to issues such as the absence of nitrate, which can be improved by tree-based modeling (Sayeed et al., 2022). The model trained in this study relies heavily on ERA5 (64 % relative contribution) with a minor contribution from MERRA-2 (36 %). Although tree-based models can improve $PM_{2.5}$ estimation accuracy and the inclusion of ERA5 meteorological features reduces the model's dependence on MERRA-2, model accuracy may decrease for areas dominated by nitrate emissions and for years before 2000.

Author contributions. SW: methodology, software, writing (original draft). MZ: visualization, validation. HuZ: data curation, methodology. PW: methodology, writing (reviewing and editing). SHK: data curation. QF: writing (reviewing and editing). CL: writing (reviewing and editing). HoZ: conceptualization, funding acquisition, supervision, writing (reviewing and editing).

References

Bai, K., Li, K., Ma, M., Li, K., Li, Z., Guo, J., Chang, N.-B., Tan, Z., and Han, D.: LGHAP: the Long-term Gap-free High-resolution Air Pollutant concentration dataset, derived via tensorflow-based multimodal data fusion, Earth Syst. Sci. Data, 14, 907–927, https://doi.org/10.5194/essd-14-907-2022, 2022.

Bai, K., Li, K., Shao, L., Li, X., Liu, C., Li, Z., Ma, M., Han, D., Sun, Y., Zheng, Z., Li, R., Chang, N.-B., and Guo, J.: LGHAP v2: a global gap-free aerosol optical depth and PM$_{2.5}$ concentration dataset since 2000 derived via big Earth data analytics, Earth Syst. Sci. Data, 16, 2425–2448, https://doi.org/10.5194/essd-16-2425-2024, 2024.

Bali, K., Dey, S., and Ganguly, D.: Diurnal patterns in ambient PM$_{2.5}$ exposure over India using MERRA-2 reanalysis data, Atmos. Environ., 248, 118180, https://doi.org/10.1016/j.atmosenv.2020.118180, 2021.

Bauer, P., Thorpe, A., and Brunet, G.: The quiet revolution of numerical weather prediction, Nature, 525, 47–55, https://doi.org/10.1038/nature14956, 2015.

Brauer, M., Guttikunda, S. K., Nishadh, K. A., Dey, S., Tripathi, S. N., Weagle, C., and Martin, R. V.: Examination of monitoring approaches for ambient air pollution: A case study for India, Atmos. Environ., 216, 116940, https://doi.org/10.1016/j.atmosenv.2019.116940, 2019.

Breiman, L.: Random Forests, Mach. Learn., 45, 5–32, https://doi.org/10.1023/A:1010933404324, 2001.

Buchard, V., Randles, C. A., da Silva, A. M., Darmenov, A., Colarco, P. R., Govindaraju, R., Ferrare, R., Hair, J., Beyersdorf, A. J., Ziemba, L. D., and Yu, H.: The MERRA-2 Aerosol Reanalysis, 1980 Onward. Part II: Evaluation and Case Studies, J. Climate, 30, 6851–6872, https://doi.org/10.1175/JCLI-D-16-0613.1, 2017.

Chen, Z., Chen, D., Zhao, C., Kwan, M.-P., Cai, J., Zhuang, Y., Zhao, B., Wang, X., Chen, B., Yang, J., Li, R., He, B., Gao, B., Wang, K., and Xu, B.: Influence of meteorological conditions on PM$_{2.5}$ concentrations across China: A review of methodology and mechanism, Environ. Int., 139, 105558, https://doi.org/10.1016/j.envint.2020.105558, 2020.

Chowdhury, S., Dey, S., Di Girolamo, L., Smith, K. R., Pillarisetti, A., and Lyapustin, A.: Tracking ambient PM$_{2.5}$ build-up in Delhi national capital region during the dry season over 15 years using a high-resolution (1 km) satellite aerosol dataset, Atmos. Environ., 204, 142–150, https://doi.org/10.1016/j.atmosenv.2019.02.029, 2019.

Dandona, L., Dandona, R., Kumar, G. A., Shukla, D., Paul, V. K., Balakrishnan, K., Prabhakaran, D., Tandon, N., Salvi, S., and Dash, A.: Nations within a nation: variations in epidemiological transition across the states of India, 1990–2016 in the Global Burden of Disease Study, Lancet, 390, 2437–2460, 2017.

Dey, S., Purohit, B., Balyan, P., Dixit, K., Bali, K., Kumar, A., Imam, F., Chowdhury, S., Ganguly, D., Gargava, P., and Shukla, V. K.: A Satellite-Based High-Resolution (1 km) Ambient PM$_{2.5}$ Database for India over Two Decades (2000–2019): Applications for Air Quality Management, Remote Sens.-Basel, 12, 3872, https://doi.org/10.3390/rs12233872, 2020.

Ganguly, T., Selvaraj, K. L., and Guttikunda, S. K.: National Clean Air Programme (NCAP) for Indian cities: Review and outlook of clean air action plans, Atmospheric Environment: X, 8, 100096, https://doi.org/10.1016/j.aeaoa.2020.100096, 2020.

Geiss, A., Silva, S. J., and Hardin, J. C.: Downscaling atmospheric chemistry simulations with physically consistent deep learning, Geosci. Model Dev., 15, 6677–6694, https://doi.org/10.5194/gmd-15-6677-2022, 2022.

Geng, G., Xiao, Q., Liu, S., Liu, X., Cheng, J., Zheng, Y., Xue, T., Tong, D., Zheng, B., and Peng, Y.: Tracking Air Pollution in China: Near Real-Time PM$_{2.5}$ Retrievals from Multisource Data Fusion, Environ. Sci. Technol., 55, 12106–12115, 2021.

Grinsztajn, L., Oyallon, E., and Varoquaux, G.: Why do tree-based models still outperform deep learning on typical tabular data?, Adv. Neur. In., 35, 507–520, 2022.

Gueymard, C. A. and Yang, D.: Worldwide validation of CAMS and MERRA-2 reanalysis aerosol optical depth products using 15 years of AERONET observations, Atmos. Environ., 225, 117216, https://doi.org/10.1016/j.atmosenv.2019.117216, 2020.

Hersbach, H., Bell, B., Berrisford, P., Hirahara, S., Horányi, A., Muñoz-Sabater, J., Nicolas, J., Peubey, C., Radu, R., Schepers, D., Simmons, A., Soci, C., Abdalla, S., Abellan, X., Balsamo, G., Bechtold, P., Biavati, G., Bidlot, J., Bonavita, M., De Chiara, G., Dahlgren, P., Dee, D., Diamantakis, M., Dragani, R., Flemming, J., Forbes, R., Fuentes, M., Geer, A., Haimberger, L., Healy, S., Hogan, R. J., Hólm, E., Janisková, M., Keeley, S., Laloyaux, P., Lopez, P., Lupu, C., Radnoti, G., de Rosnay, P., Rozum, I., Vamborg, F., Villaume, S., and Thépaut, J.-N.: The ERA5 global reanalysis, Q. J. Roy. Meteor. Soc., 146, 1999–2049, https://doi.org/10.1002/qj.3803, 2020.

Hu, X., Chu, L., Pei, J., Liu, W., and Bian, J.: Model complexity of deep learning: a survey, Knowl. Inf. Syst., 63, 2585–2619, https://doi.org/10.1007/s10115-021-01605-0, 2021.

Huang, C., Hu, J., Xue, T., Xu, H., and Wang, M.: High-Resolution Spatiotemporal Modeling for Ambient PM$_{2.5}$ Exposure Assessment in China from 2013 to 2019, Environ. Sci. Technol., 55, 2152–2162, 2021.

Huang, J., Zhou, Y., and Yong, W.-A.: Data-driven discovery of multiscale chemical reactions governed by the law of mass action, J. Comput. Phys., 448, 110743, https://doi.org/10.1016/j.jcp.2021.110743, 2022.

Huang, Y. and Seinfeld, J. H.: A neural network-assisted Euler integrator for stiff kinetics in atmospheric chemistry, Environ. Sci. Technol., 56, 4676–4685, 2022.

Jabbar, H. and Khan, R. Z.: Methods to avoid over-fitting and under-fitting in supervised machine learning (comparative study), Computer Science, Communication and Instrumentation Devices, 70, 978–981, 2015.

Katoch, V., Kumar, A., Imam, F., Sarkar, D., Knibbs, L. D., Liu, Y., Ganguly, D., and Dey, S.: Addressing Biases in Ambient PM$_{2.5}$ Exposure and Associated Health Burden Estimates by Filling Satellite AOD Retrieval Gaps over India, Environ. Sci. Technol., 57, 19190–19201, https://doi.org/10.1021/acs.est.3c03355, 2023.

Ke, G. L., Meng, Q., Finley, T., Wang, T. F., Chen, W., Ma, W. D., Ye, Q. W., and Liu, T. Y.: LightGBM: A Highly Efficient Gradient Boosting Decision Tree, 31st Annual Conference on Neural Information Processing Systems (NIPS), Long Beach, CA, Dec 04-09, WOS:000452649403021, 2017.

Kumar, V., Malyan, V., Sahu, M., Biswal, B., Pawar, M., and Dev, I.: Spatiotemporal analysis of fine particulate mat-

ter for India (1980–2021) from MERRA-2 using ensemble machine learning, Atmos. Pollut. Res., 14, 101834, https://doi.org/10.1016/j.apr.2023.101834, 2023.

Kumari, S., Verma, N., Lakhani, A., and Kumari, K. M.: Severe haze events in the Indo-Gangetic Plain during post-monsoon: Synergetic effect of synoptic meteorology and crop residue burning emission, Sci. Total Environ., 768, 145479, https://doi.org/10.1016/j.scitotenv.2021.145479, 2021.

Li, H., Yang, Y., Wang, H., Li, B., Wang, P., Li, J., and Liao, H.: Constructing a spatiotemporally coherent long-term $PM_{2.5}$ concentration dataset over China during 1980–2019 using a machine learning approach, Sci. Total Environ., 765, 144263, https://doi.org/10.1016/j.scitotenv.2020.144263, 2021.

Li, T., Zhang, Q., Peng, Y., Guan, X., Li, L., Mu, J., Wang, X., Yin, X., and Wang, Q.: Contributions of Various Driving Factors to Air Pollution Events: Interpretability Analysis from Machine Learning Perspective, Environ. Int., 173, 107861, https://doi.org/10.1016/j.envint.2023.107861, 2023.

Liang, W., Luo, S., Zhao, G., and Wu, H.: Predicting hard rock pillar stability using GBDT, XGBoost, and LightGBM algorithms, Mathematics, 8, 765, https://doi.org/10.3390/math8050765, 2020.

Ma, Z., Dey, S., Christopher, S., Liu, R., Bi, J., Balyan, P., and Liu, Y.: A review of statistical methods used for developing large-scale and long-term $PM_{2.5}$ models from satellite data, Remote Sens. Environ., 269, 112827, https://doi.org/10.1016/j.rse.2021.112827, 2022.

Maheshwarkar, P., Ralhan, A., Sunder Raman, R., Tibrewal, K., Venkataraman, C., Dhandapani, A., Kumar, R. N., Mukherjee, S., Chatterje, A., Rabha, S., Saikia, B. K., Bhardwaj, A., Chaudhary, P., Sinha, B., Lokhande, P., Phuleria, H. C., Roy, S., Imran, M., Habib, G., Azharuddin Hashmi, M., Qureshi, A., Qadri, A. M., Gupta, T., Lian, Y., Pandithurai, G., Prasad, L., Murthy, S., Deswal, M., Laura, J. S., Chhangani, A. K., Najar, T. A., and Jehangir, A.: Understanding the Influence of Meteorology and Emission Sources on $PM_{2.5}$ Mass Concentrations Across India: First Results From the COALESCE Network, J. Geophys. Res.-Atmos., 127, e2021JD035663, https://doi.org/10.1029/2021JD035663, 2022.

Maji, K. J., Namdeo, A., and Bramwell, L.: Driving factors behind the continuous increase of long-term $PM_{2.5}$-attributable health burden in India using the high-resolution global datasets from 2001 to 2020, Sci. Total Environ., 866, 161435, https://doi.org/10.1016/j.scitotenv.2023.161435, 2023.

Martin, R. V., Brauer, M., van Donkelaar, A., Shaddick, G., Narain, U., and Dey, S.: No one knows which city has the highest concentration of fine particulate matter, Atmospheric Environment: X, 3, 100040, https://doi.org/10.1016/j.aeaoa.2019.100040, 2019.

Muñoz-Sabater, J., Dutra, E., Agustí-Panareda, A., Albergel, C., Arduini, G., Balsamo, G., Boussetta, S., Choulga, M., Harrigan, S., Hersbach, H., Martens, B., Miralles, D. G., Piles, M., Rodríguez-Fernández, N. J., Zsoter, E., Buontempo, C., and Thépaut, J.-N.: ERA5-Land: a state-of-the-art global reanalysis dataset for land applications, Earth Syst. Sci. Data, 13, 4349–4383, https://doi.org/10.5194/essd-13-4349-2021, 2021.

Murray, C. J., Aravkin, A. Y., Zheng, P., Abbafati, C., Abbas, K. M., Abbasi-Kangevari, M., Abd-Allah, F., Abdelalim, A., Abdollahi, M., and Abdollahpour, I. J. T. L.: Global burden of 87 risk factors in 204 countries and territories, 1990–2019: a systematic analysis for the Global Burden of Disease Study 2019, Lancet, 396, 1223–1249, 2020.

Nagpure, A. S., Ramaswami, A., and Russell, A.: Characterizing the spatial and temporal patterns of open burning of municipal solid waste (MSW) in Indian cities, Environ. Sci. Technol., 49, 12904–12912, 2015.

Navinya, C. D., Vinoj, V., and Pandey, S. K.: Evaluation of $PM_{2.5}$ Surface Concentrations Simulated by NASA's MERRA Version 2 Aerosol Reanalysis over India and its Relation to the Air Quality Index, Aerosol Air Qual. Res., 20, 1329–1339, https://doi.org/10.4209/aaqr.2019.12.0615, 2020.

Ni, Y., Yang, Y., Wang, H., Li, H., Li, M., Wang, P., Li, K., and Liao, H.: Contrasting changes in ozone during 2019–2021 between eastern and the other regions of China attributed to anthropogenic emissions and meteorological conditions, Sci. Total Environ., 908, 168272, https://doi.org/10.1016/j.scitotenv.2023.168272, 2024.

Pandey, A., Sadavarte, P., Rao, A. B., and Venkataraman, C.: Trends in multi-pollutant emissions from a technology-linked inventory for India: II. Residential, agricultural and informal industry sectors, Atmos. Environ., 99, 341–352, https://doi.org/10.1016/j.atmosenv.2014.09.080, 2014.

Pandey, A., Brauer, M., Cropper, M. L., Balakrishnan, K., Mathur, P., Dey, S., Turkgulu, B., Kumar, G. A., Khare, M., and Beig, G.: Health and economic impact of air pollution in the states of India: the Global Burden of Disease Study 2019, The Lancet Planetary Health, 5, e25–e38, 2021.

Pant, P., Lal, R. M., Guttikunda, S. K., Russell, A. G., Nagpure, A. S., Ramaswami, A., and Peltier, R. E.: Monitoring particulate matter in India: recent trends and future outlook, Air Qual. Atmos. Hlth., 12, 45–58, 2019.

Ren, J., Zhang, M., Yu, C., and Liu, Z.: Balanced mse for imbalanced visual regression, Proceedings of the IEEE/CVF Conference on Computer Vision and Pattern Recognition, 21–24 June 2022, New Orleans Ernest N. Morial Convention Center, New Orleans, Louisiana, 7926–7935, https://arxiv.org/abs/2203.16427 (last access: 30 July 2024), 2022.

Ren, X., Mi, Z., Cai, T., Nolte, C. G., and Georgopoulos, P. G.: Flexible Bayesian Ensemble Machine Learning Framework for Predicting Local Ozone Concentrations, Environ. Sci. Technol., 56, 3871–3883, https://doi.org/10.1021/acs.est.1c04076, 2022.

Sayeed, A., Lin, P., Gupta, P., Tran, N. N. M., Buchard, V., and Christopher, S.: Hourly and Daily $PM_{2.5}$ Estimations Using MERRA-2: A Machine Learning Approach, Earth Space Sci., 9, e2022EA002375, https://doi.org/10.1029/2022EA002375, 2022.

Shi, G., Lu, X., Deng, Y., Urpelainen, J., Liu, L.-C., Zhang, Z., Wei, W., and Wang, H.: Air pollutant emissions induced by population migration in China, Environ. Sci. Technol., 54, 6308–6318, 2020.

Stirnberg, R., Cermak, J., Kotthaus, S., Haeffelin, M., Andersen, H., Fuchs, J., Kim, M., Petit, J.-E., and Favez, O.: Meteorology-driven variability of air pollution (PM_1) revealed with explainable machine learning, Atmos. Chem. Phys., 21, 3919–3948, https://doi.org/10.5194/acp-21-3919-2021, 2021.

Sun, X., Liu, M., and Sima, Z.: A novel cryptocurrency price trend forecasting model based on LightGBM, Financ. Res. Lett., 32, 101084, https://doi.org/10.1016/j.frl.2018.12.032, 2020.

Tiwari, S., Srivastava, A. K., Bisht, D. S., Parmita, P., Srivastava, M. K., and Attri, S.: Diurnal and seasonal variations of black carbon

and PM$_{2.5}$ over New Delhi, India: Influence of meteorology, Atmos. Res., 125, 50–62, 2013.

Upadhyay, A., Dey, S., and Goyal, P.: A comparative assessment of regional representativeness of EDGAR and ECLIPSE emission inventories for air quality studies in India, Atmos. Environ., 223, 117182, https://doi.org/10.1016/j.atmosenv.2019.117182, 2020.

van Donkelaar, A., Hammer, M. S., Bindle, L., Brauer, M., Brook, J. R., Garay, M. J., Hsu, N. C., Kalashnikova, O. V., Kahn, R. A., Lee, C., Levy, R. C., Lyapustin, A., Sayer, A. M., and Martin, R. V.: Monthly Global Estimates of Fine Particulate Matter and Their Uncertainty, Environ. Sci. Technol., 55, 15287–15300, https://doi.org/10.1021/acs.est.1c05309, 2021.

Vos, T., Lim, S. S., Abbafati, C., Abbas, K. M., Abbasi, M., Abbasifard, M., Abbasi-Kangevari, M., Abbastabar, H., Abd-Allah, F., and Abdelalim, A.: Global burden of 369 diseases and injuries in 204 countries and territories, 1990–2019: a systematic analysis for the Global Burden of Disease Study 2019, Lancet, 396, 1204–1222, 2020.

Wang, K. C., Dickinson, R. E., Wild, M., and Liang, S.: Atmospheric impacts on climatic variability of surface incident solar radiation, Atmos. Chem. Phys., 12, 9581–9592, https://doi.org/10.5194/acp-12-9581-2012, 2012.

Wang, S., Kota, S. H., and Zhang, H.: LongPMInd: long-term (1980–2022) daily ground particulate matter datasets in India, Zenodo [data set], https://doi.org/10.5281/zenodo.10073944, 2023a.

Wang, S., Wang, P., Qi, Q., Wang, S., Meng, X., Kan, H., Zhu, S., and Zhang, H.: Improved estimation of particulate matter in China based on multisource data fusion, Sci. Total Environ., 869, 161552, https://doi.org/10.1016/j.scitotenv.2023.161552, 2023b.

Wang, S., Wang, P., Zhang, R., Meng, X., Kan, H., and Zhang, H.: Estimating particulate matter concentrations and meteorological contributions in China during 2000–2020, Chemosphere, 330, 138742, https://doi.org/10.1016/j.chemosphere.2023.138742, 2023c.

Wang, S., Zhang, M., Gao, Y., Wang, P., Fu, Q., and Zhang, H.: Diagnosing drivers of PM$_{2.5}$ simulation biases from meteorology, chemical composition, and emission sources using an efficient machine learning method, EGUsphere [preprint], https://doi.org/10.5194/egusphere-2023-1531, 2023d.

Wei, J., Li, Z., Lyapustin, A., Sun, L., Peng, Y., Xue, W., Su, T., and Cribb, M.: Reconstructing 1-km-resolution high-quality PM$_{2.5}$ data records from 2000 to 2018 in China: spatiotemporal variations and policy implications, Remote Sens. Environ., 252, 112136, https://doi.org/10.1016/j.rse.2020.112136, 2021a.

Wei, J., Li, Z., Pinker, R. T., Wang, J., Sun, L., Xue, W., Li, R., and Cribb, M.: Himawari-8-derived diurnal variations in ground-level PM$_{2.5}$ pollution across China using the fast space-time Light Gradient Boosting Machine (LightGBM), Atmos. Chem. Phys., 21, 7863–7880, https://doi.org/10.5194/acp-21-7863-2021, 2021b.

Wei, J., Li, Z., Lyapustin, A., Wang, J., Dubovik, O., Schwartz, J., Sun, L., Li, C., Liu, S., and Zhu, T.: First close insight into global daily gapless 1 km PM$_{2.5}$ pollution, variability, and health impact, Nat. Commun., 14, 8349, https://doi.org/10.1038/s41467-023-43862-3, 2023.

Yan, J., Xu, Y., Cheng, Q., Jiang, S., Wang, Q., Xiao, Y., Ma, C., Yan, J., and Wang, X.: LightGBM: accelerated genomically designed crop breeding through ensemble learning, Genome Biol., 22, 1–24, 2021.

Yang, X., Zhao, C. F., Zhou, L. J., Wang, Y., and Liu, X. H.: Distinct impact of different types of aerosols on surface solar radiation in China, J. Geophys. Res.-Atmos., 121, 6459–6471, https://doi.org/10.1002/2016jd024938, 2016.

Yang, Y., Zha, K., Chen, Y., Wang, H., and Katabi, D.: Delving into deep imbalanced regression, International Conference on Machine Learning, 18–24 July 2021, Honolulu, Hawaii, 65 USA, 11842–11851, https://arxiv.org/abs/2102.09554 (last access: 30 July 2024), 2021.

Ying, X.: An overview of overfitting and its solutions, J. Phys. Conf. Ser., 1168, 022022, https://doi.org/10.1088/1742-6596/1168/2/022022, 2019.

Yu, W., Ye, T., Zhang, Y., Xu, R., Lei, Y., Chen, Z., Yang, Z., Zhang, Y., Song, J., and Yue, X.: Global estimates of daily ambient fine particulate matter concentrations and unequal spatiotemporal distribution of population exposure: a machine learning modelling study, The Lancet Planetary Health, 7, e209–e218, 2023.

Zhang, T. N., He, W. H., Zheng, H., Cui, Y. P., Song, H. Q., and Fu, S. L.: Satellite-based ground PM$_{2.5}$ estimation using a gradient boosting decision tree, Chemosphere, 268, 128801, https://doi.org/10.1016/j.chemosphere.2020.128801, 2021.